The bistable, but non-oscillatory electrochemical system with the negative differential resistance (NDR) generated by the potential-dependent convection at the liquid electrode|solution interface.

Marek Orlik, Maciej T. Gorzkowski, Rafał Jurczakowski
Laboratory of Electroanalytical Chemistry, Faculty of Chemistry, The University of Warsaw, Ul. Pasteura 1, 02-093 Warsaw, POLAND
Email: morlik@chem.uw.edu.pl

Convection as a non-linear dynamical phenomenon is still a subject of intensive experimental and theoretical studies in both physics and chemistry. Remarkable universalities (as e.g. hexagonal cells) were found in convective motions in various systems, with different driving forces operating.

In electrochemical systems the convection can be caused either by density gradients, or by electrohydrodynamic forces, or by the surface tension gradients appearing at the surfaces of liquid electrodes, in all cases as a phenomenon accompanying the electrolysis. For the electroreduction of Hg(II) ions at the Hg electrode the self-induced convection may temporarily take a form of self-organized cellular patterns [1].

In our recent studies we investigated the electrochemical characteristics of the latter process [2] and analyzed the observed phenomena with standard techniques of nonlinear dynamics [3]. In this case the electric current is strongly enhanced by the convective transport of Hg(II) ions from the solution bulk to the electrode surface. The rate of this convection is in turn strongly dependent on the imposed electrode potential: it passes through the maximum, and when it decreases, the region of the *N*-shaped negative differential resistance (N-NDR) develops on the current-potential characteristics (Figure 1).

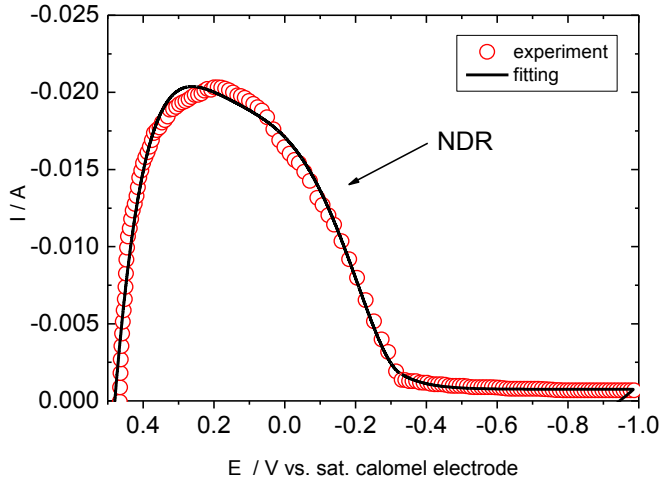

Figure 1. Experimental quasi-steady state *I-E* characteristics of the Hg(II) electroreduction at the flat Hg electrode (A = 3.3 cm^2) under conditions when the convection sets in at positive potentials and passes through the maximum as a function of increasing negative electrode potential.

Since the NDR systems are expected to exhibit bistability and oscillations, *which were however never studied before for this particular system*, we undertook respective experimental and theoretical investigations. The destabilization of the N-NDR systems

requires appropriate ohmic drops, i.e. inserting of adjustable external ohmic resistance in the electric circuit of the working electrode (Figure 2):

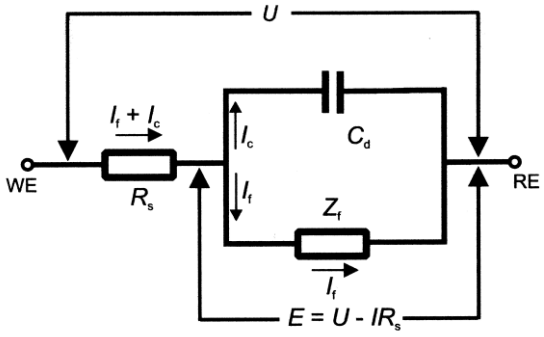

Fig. 2. Schematic equivalent electric circuit for the electroreduction of Hg(II) at the Hg electrode: Z_f, I_f – the faradaic impedance of the electrode process and the associated faradaic current, respectively; I_c – capacitive current, associated with the charging of the electric double layer at the solution|electrode interface; R_s – external resistor in the circuit of the working electrode (WE); RE – reference (saturated calomel) electrode; U - externally applied voltage, E – the effective potential of the working electrode. The electrochemical system itself may exhibit certain uncompensated resistance (solution resistance) R_u which yields R_s+R_u as a total serial resistance.

We studied the dynamical instabilities in the Hg(II) + 2e = Hg process, for varying external voltages U and serial resistances R_s, with the intention to construct the experimental bifurcation diagram. In spite of certain drift of the steady-state characteristics we were able to detect the hysteresis of the current I vs. cyclic variations of the voltage U (i.e. **bistability**, see Figure 3), but **no spontaneous oscillations** of the current were observed [2].

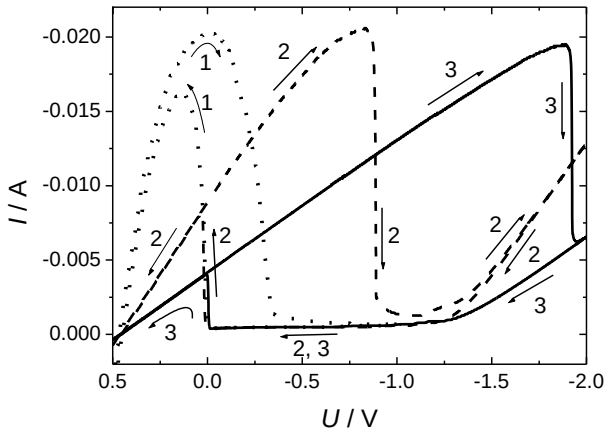

Figure 3. Hysteresis (bistability) in the *I-U* characteristics upon the cyclic changes of the external voltage U during the electroreduction of Hg(II) at the flat Hg electrode, for different total serial resistances of the circuit: (1) R_u = 10 Ω , R_s = 0 (no externally applied resistance), (2) (R_u + R_s) = 50 Ω, (3) (R_u + R_s) = 100 Ω. Curve (1) shows a distinct NDR region which in curves (2, 3) turns into the bistable (hysteresis) regions, indicating the destabilization of the steady-states from curve (1) through the saddle-node bifurcations. **High currents** correspond to **self-induced convection**, while ***low*** currents correspond to ***quiescent mercury surface***, thus it is the bistability between the convection and the convection-less regime [2].

In order to find out whether the observed characteristics are reliable, we constructed the theoretical model of the process studied. The following assumptions were made [3]:

(i) the faradaic current of the Hg(II) electroreduction is approximated by the dependence invoking the concept of the linear (Nernst) diffusion layer of a thickness δ:

$$I_f(E) = -nFAD_{ox}\left(\frac{\partial c_{ox}}{\partial x}\right)_0 \approx -nFAD_{ox}\left(\frac{c_{ox}^0 - c_{ox}(0,t)}{\delta}\right)_0 \quad (1)$$

with n – number of electrons exchanged, F – Faraday constant, A – electrode surface area, D_{ox} – diffusion coefficient of the reducible Ox (i.e. Hg(II)) species, with its concentration equal to c_{ox}^0 in the solution bulk and equal to $c_{ox}(0,t)$ at the electrode surface;

(ii) since for the electrode potentials applied the concentration of Hg(II) at the electrode surface $c_{ox}(0,t) \approx 0$, Equation (1) simplifies to the form:

$$I_f(E) \approx -nFAD_{ox}\frac{c_{ox}^0}{\delta} \quad (2)$$

(iii) as a consequence, the observed I=f(E) dependences (like that in Fig. 1) are interpreted in terms of variation of only the Nernst diffusion layer δ with E, according to Figure 4:

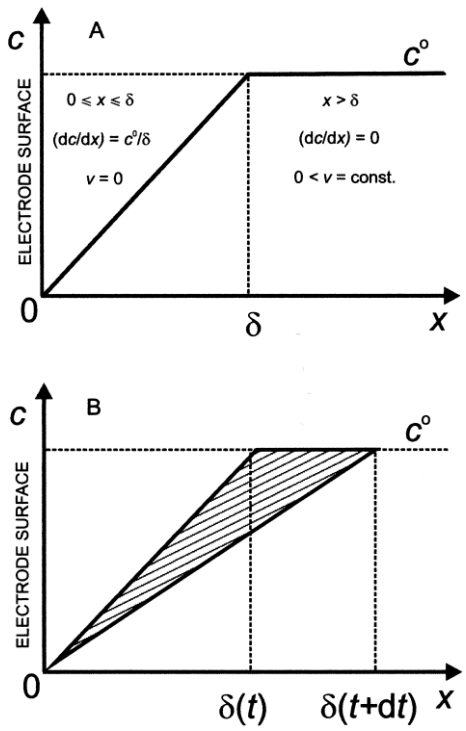

Figure 4. (A) The linearized concentration profile for the conditions where convection of the velocity v affects the thickness of the Nernst diffusion layer (δ) and thus the faradaic current, with zero surface concentration of Ox species imposed ($c_{ox}(x=0, t) = 0$). For simplicity the component of the fluid velocity, normal to the electrode surface, was assumed constant throughout the solution outside the Nernst layer; (B) Schematic picture of the variations of the thickness of the linearized Nernst diffusion layer, explaining the variation of the current I [3].

(iv) the effective electrode potential E and the thickness of the diffusion layer δ were chosen as the **two dynamical variables**. Based on the charge conservation principle and quantitative balance of a transport of Hg(II) in the diffusion layer the following equations describing the dynamics of our electrochemical systems were derived [3]:

$$\frac{\mathrm{d}E}{\mathrm{d}t} = \frac{U - E}{C_\mathrm{d} A R_\mathrm{s}} + \frac{nFD_\mathrm{ox}c^0_\mathrm{ox}}{C_\mathrm{d}\delta} \equiv f(E,\delta) \tag{3}$$

$$\frac{\mathrm{d}\delta}{\mathrm{d}t} = \frac{2D_\mathrm{ox}}{\delta} - 2v(E) \equiv g(E,\delta) \tag{4}$$

The stability analysis was performed [3] for the linearized equations (3, 4):

$$\frac{\mathrm{d}E}{\mathrm{d}t} = \left(\frac{\partial f}{\partial E}\right)_\mathrm{ss}(E - E_\mathrm{ss}) + \left(\frac{\partial f}{\partial \delta}\right)_\mathrm{ss}(\delta - \delta_\mathrm{ss}) = \left(\frac{-1}{C_\mathrm{d} A R_\mathrm{s}}\right)_\mathrm{ss}(E - E_\mathrm{ss}) - \left(\frac{nFD_\mathrm{ox}c^0_\mathrm{ox}}{C_\mathrm{d}\delta^2}\right)_\mathrm{ss}(\delta - \delta_\mathrm{ss}) \tag{5}$$

$$\frac{\mathrm{d}\delta}{\mathrm{d}t} = \left(\frac{\partial g}{\partial E}\right)_\mathrm{ss}(E - E_\mathrm{ss}) + \left(\frac{\partial g}{\partial \delta}\right)_\mathrm{ss}(\delta - \delta_\mathrm{ss}) = -2\left(\frac{\mathrm{d}v}{\mathrm{d}E}\right)_\mathrm{ss}(E - E_\mathrm{ss}) - \left(\frac{2D_\mathrm{ox}}{\delta^2}\right)_\mathrm{ss}(\delta - \delta_\mathrm{ss}) \tag{6}$$

which generated the corresponding Jacobi matrix:

$$\mathbf{J} = \begin{bmatrix} \left(\frac{\partial f}{\partial E}\right)_\mathrm{ss} & \left(\frac{\partial f}{\partial \delta}\right)_\mathrm{ss} \\ \left(\frac{\partial g}{\partial E}\right)_\mathrm{ss} & \left(\frac{\partial g}{\partial \delta}\right)_\mathrm{ss} \end{bmatrix} = \begin{bmatrix} \frac{-1}{C_\mathrm{d} A R_\mathrm{s}} & -\left(\frac{nFDc^0_\mathrm{ox}}{C_\mathrm{d}\delta^2}\right)_\mathrm{ss} \\ -2\left(\frac{\mathrm{d}v}{\mathrm{d}E}\right)_\mathrm{ss} & -\left(\frac{2D_\mathrm{ox}}{\delta^2}\right)_\mathrm{ss} \end{bmatrix} \tag{7}$$

with the trace and the determinant given by:

$$Tr(\mathbf{J}) = \left[\frac{-1}{C_\mathrm{d} A R_\mathrm{s}} - \left(\frac{2D_\mathrm{ox}}{\delta^2}\right)_\mathrm{ss}\right] \tag{8}$$

$$Det(\mathbf{J}) = \left[\frac{1}{C_\mathrm{d} A R_\mathrm{s}}\right]\left[\frac{2D_\mathrm{ox}}{\delta^2}\right]_\mathrm{ss} - 2\left(\frac{nFD_\mathrm{ox}c^0_\mathrm{ox}}{C_\mathrm{d}\delta^2}\right)\left(\frac{\mathrm{d}v}{\mathrm{d}E}\right)_\mathrm{ss} = \left[\frac{1}{R_\mathrm{s}} + \left(\frac{\mathrm{d}I}{\mathrm{d}E}\right)_\mathrm{ss}\right]\left[\frac{2D_\mathrm{ox}}{C_\mathrm{d} A \delta^2}\right]_\mathrm{ss} \tag{9}$$

The saddle node bifurcation occurs for *Det*(**J**)=0, while the Hopf bifurcation requires that the conditions: *Tr*(**J**)=0 with *Det*(**J**)>0 are met.

From Equation (8) it follows that in terms of our simple model the condition *Tr*(**J**)=0 is **never met** in this case, and thus the oscillations originating through the Hopf bifurcation **are not possible**. The latter conclusion is thus in line with the experimentally observed lack of oscillations. Formally, this situation occurs because the a_{11} element of the Jacobi matrix (7), being the $\partial/\partial \mathrm{E}[\mathrm{d}E/\mathrm{d}t]$ expression, is always negative, so the electrode potential *E* in this system is **NOT an autocatalytic variable**, contrary to the systems in which the current is controlled not only by the rate of transport, but also by rate of the proper electron-transfer step at the electrode|solution interface.

The theoretical bifurcation diagram based on *Det*(**J**)=0 is shown in Figure 5, while Fig. 6 shows the exemplary nullclines of Equations (3, 4), corresponding to the bistable behavior.

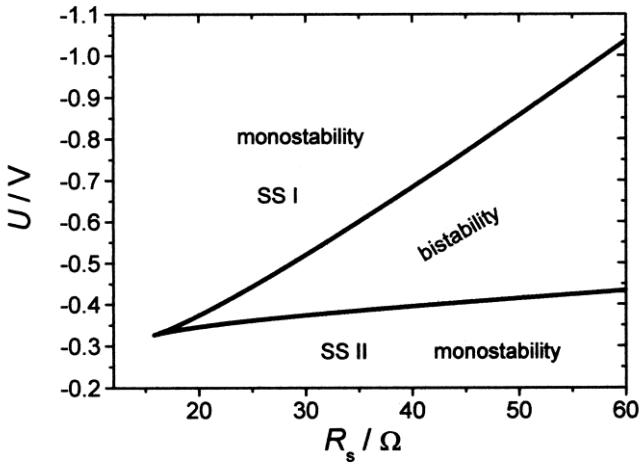

Figure 5. Bifurcation diagram of Equations (3, 4) showing the points of saddle-node bifurcations for the range of (U, R_s) parameters, used in our experiments. There are no points of the Hopf bifurcations present.

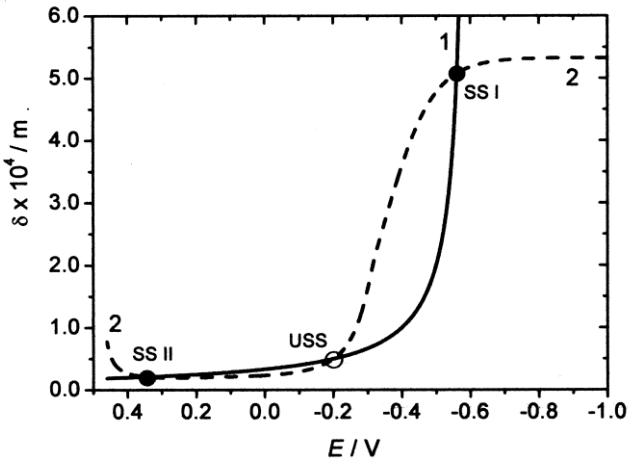

Figure 6. Nullclines of Equations (3, 4), corresponding to the condition dE/dt=0 (curve 1) and dδ/dt = 0 (curve 2) for U = -0.6 V and R_s = 50 Ω (bistable regime). Filled circles denote the stable steady-states (SS I, SS II), while the hollow circle – the unstable steady-state (USS).

A **relative importance** of the presented analysis may be summarized in the following way. The N-NDR electrochemical systems usually exhibit oscillations and bistability, for the appropriate range of external voltages U and serial resistance R_s. The system described in this presentation is a **RARE example** of the N-NDR system, the dynamical characteristics of which **do not allow oscillatory behavior** through the Hopf bifurcation.

References:

[1] R. Aogaki, K. Kitazawa, K. Fueki, T. Mukaibo, Electrochim. Acta, 23 (1978) 867 - 874
[2] M. T. Gorzkowski, R. Jurczakowski, M. Orlik, J. Electroanal. Chem., 615 (2008) 135-144
[3] M. Orlik, M. T. Gorzkowski, J. Electroanal. Chem., 617 (2008) 64-70